# Predictive Model of the Mechanical Behaviour of a Composite Structure With Integrated Photovoltaic Cells for Automotive Application

**Tatiana Duigou** ( tatiana.duigou@cea.fr )
Universit e Grenoble Alpes, CEA, LITEN, DTS, SMPV, LMPI, INES, F-38000 Grenoble, France
https://orcid.org/0000-0003-2416-6155
**Manuel Lagache**
SYMME, Université Savoie Mont Blanc
**Philippe Saffré**
SYMME, Université Savoie Mont Blanc
**Julien Gaume**
Université Grenoble Alpes, CEA, LITEN, DTS, SMPV, LMPI
**Fabien Chabuel**
Université Grenoble Alpes, CEA, LITEN, DTS, SMPV, LMPI
**Lionel Tenchine**
Centre Technique Industriel de la Plasturgie et des Composites (IPC)
**Georges Habchi**
SYMME, Université Savoie Mont Blanc

**Research**

**Keywords:** Vehicle-Integrated PhotoVoltaics, compositronics, modelling, qualification and testing, design

**Posted Date:** October 19th, 2020

**DOI:** https://doi.org/10.21203/rs.3.rs-93090/v1

RESEARCH

# Predictive model of the mechanical behaviour of a composite structure with integrated photovoltaic cells for automotive application

Tatiana Duigou[1,2*], Manuel Lagache[2], Philippe Saffré[2], Julien Gaume[1], Fabien Chabuel[1], Lionel Tenchine[3] and Georges Habchi[2]

*Correspondence: tatiana.duigou@cea.fr
[1]Université Grenoble Alpes, CEA, LITEN, DTS, SMPV, LMPI, INES, F-38000 Grenoble, France
Full list of author information is available at the end of the article

**Abstract**

The end of the use of internal combustion engines is scheduled for 2035 in the US and 2040 in France. These evolutions will require Electric Vehicles (EVs) to evolve significantly. In this context, the use of PV modules is one of the alternatives considered to make vehicles partially energy self-sufficient and limit the size of the batteries. However, this integration should not be at the expense of the mechanical behaviour of the car parts. An optimization of this integration is therefore necessary. To optimize the mechanical behaviour of the structure in regard with standards, the development of a numerical model is proposed. This model of a one-cell panel is validated through experimental tests, and further used to optimize the stack using a Design Of Experiment (DOE) method. The optimized sample including solar cells is 2.7 times lighter than an equivalent automotive part made of steel.

**Keywords:** Vehicle-Integrated PhotoVoltaics; compositronics; modelling; qualification and testing; design

## Introduction

Greenhouse gas emissions have almost doubled since 1970 and the transport sector emits 14% of these emissions. Consequently, the automotive sector is encouraged to propose alternative solutions to gas-powered vehicles. The current trend to tackle this issue is to electrify vehicles, usually using high capacity batteries. However, these popular technologies of EVs require a large amount of lithium for their heavy batteries. Thus, the integration of PhotoVoltaic (PV) modules as body parts for hybrid or electric vehicles could allow several improvements compared to non-solarized EVs. Other advantages include the reduction of the battery size or the possibility to provide power for the additional equipment [1].

Automotive manufacturers already developed a large amount of PV panels integrated into cars. Most of these technologies utilize materials traditionally used in the PV industry: glass or polymers like polycarbonate. However, the mechanical requirements for automotive parts imply that the body parts need to withstand a set of loads, to which polymer PV panels are not suited. Moreover, as it is supposed to provide energy to the vehicle, the integration of photovoltaic cells should not penalize the weight of the vehicle so as to maximize the vehicle range allowed by the energy intake of the PV module. Glass PV panels do not tackle this issue. For

these mechanical and weight reasons, composites seem to be an interesting alternative for the front and backsheet materials. However, to keep a competitive product, the design of the composite structure integrating PV should guaranty the previous specifications and minimize the strain and residual stresses due to the heterogeneity and non-symmetry of the structure [2, 3, 4].

The determination of elastic deformations in PV laminates is a prerequisite to propose new technical solutions that may result in innovative solar panel design. Though many works already simulate the mechanical behaviour of traditional PV modules [4, 5, 3], none has been found to model composite modules integrating PV cells. In this context, a Finite Element (FE) model simulating the mechanical behaviour of a one-cell composite PV module has been developed. Moreover, an analytical model obtained by the DOE method has been developed to understand the roles played by the different materials on the global mechanical behaviour. This analytical model will further enable an optimization of the structure.

First, the FE model developed is described. Further, experimental tests led to provide materials properties and to validate this numerical model are explained. They are compared to the numerical simulation results. Finally, the DOE method used to optimize the mass and rigidity of the composite PV panel is developed.

## Numerical model

The numerical model is designed with a FE analysis software -ANSYS- to describe a module integrating a solar cell in sheets of polymer encapsulant. It uses around 5500 hexahedral solid elements with adapted sizing. The numerical resolution uses a linear elastic model.

The pattern is composed of one cell with copper ribbons on the front face (figure 1). It is representative of a 4-cell module. This is the intermediate step before taking also into account the interconnections between cells. The front sheet and back sheet are made of glass fibre-based composite materials withstanding the loads and protecting the cells from the environment. The data for the epoxy/glass fibre fabrics were characterized through tensile, density and fibre mass ratio measurements. Factors values like Poisson ratio of composite plies, and data for copper ribbons were found either in the materials datasheets or in the literature [6] [7]. The data for encapsulants had already been measured at CEA in previous studies [8]. The model for PV cells is Silicon Anistropic from ANSYS engineering materials library. All material properties can be found in tables 1 and 2. The matrix of anisotropic elasticity of silicon is in table 3.

**Table 1 Properties of the 3 tested composite materials at $20^oC$.**

| Measurement | Unit | Material A | Material B | Material C |
|---|---|---|---|---|
| Density | $kg/m^3$ | $1,483$ | $1,490$ | $1,793$ |
| Fibre volume ratio | % | 39.2 | 27.7 | 43.3 |
| Poisson ratio XY | | 0.3 | 0.3 | 0.3 |
| Young modulus | *GPa* | $12.423 \pm 1.203$ | X: $11.103 \pm 1.104$, Y:$11.992 \pm 1.367$ | $18.817 \pm 1.999$ |

**Table 2 Properties of the non composite materials at $20^oC$.**

| Measurement | Unit | PV cell | Copper | Encapsulant D | Encapsulant E |
|---|---|---|---|---|---|
| Density | $kg/m^3$ | 2,330 | 10,470 | 935 | 950 |
| Poisson ratio | % | | 0.365 | 0.49 | 0.49 |
| Young modulus | *GPa* | See matrix of anisotropic elasticity | 69 | 0.022 | 0.477 |

**Table 3 Properties of the Anisotropic Silicon at $20^oC$ in GPa (ANSYS material property).**

| | | | | | |
|---|---|---|---|---|---|
| 166 | | | | | |
| 64 | 166 | | | | |
| 64 | 64 | 166 | | | |
| 0 | 0 | 0 | 80 | | |
| 0 | 0 | 0 | 0 | 80 | |
| 0 | 0 | 0 | 0 | 0 | 80 |

The setting up of the test is also adapted for a parametric analysis exploring the influence of materials, thickness, ply orientations, number of plies... on the stiffness of the whole structure. This parametrization enables an optimization of this non-symmetric structure to provide a bending stiffness equivalent to that of a car roof while minimizing the weight. The parametrical aspect is combined with a DOE method to scan a large number of configurations and to identify the most critical parameters among the number of plies, their orientation, the nature of the composite fabric and of the encapsulant.

## Experimental tests

This model is validated by a set of experiments on panels of dimensions 20 cm x 20 cm. Two types of samples have been produced: type 1 with vacuum bagging process, using materials A and B for the composite plies, and type 2 with lamination process and material C for the composite stack. Various materials have been used, including:

- Different glass fibre fabrics combined with epoxy resin for the front and back sheets. They will be named materials A, B and C.
- Different encapsulants, including cross-linked and thermoplastic encapsulants. They will be called encapsulants D and E.

Several tests have been performed. The first ones aimed at characterizing the properties of the composite plies: density measurements, fibre volume ratio measurements, tensile tests. The other ones were 3-point bending tests, to validate the mechanical behaviour of the stack.

### Density measurements

The density measurements were performed with a Ohaus density determination kit. Three samples were tested for each material. The densities of the 3 tested materials can be found in table 1.

### Fibre ratio measurements

These measurements were performed by fibre mass ratio tests at $625^o$C [9]. One sample of dimensions 2*2 cm was tested for each material. The fibre volume ratios of the 3 tested materials can be found in table 1.

### Tensile tests

These tests aimed at characterizing the mechanical properties of the different epoxy/glass-fibre fabrics envisaged for the optimization of the stack. The tensile test machine is a Shimadzu AG-XD 50 plus with a 1 KN sensor. The displacement measurements are coming from the TRViewX non-contact digital video extensometer.

The tensile tests enable to obtain the elastic moduli of the different materials envisaged for the stack. The tests were performed on 3 different composite materials. The tensile curves for material C is displayed in figure 2. The dispersion of the results is probably related to differences in the parallelism of the fibres in the tensile direction, for some samples. The averages of the elastic moduli for the samples are transcribed in table 1. These data fed the mechanical properties of the materials in the finite element model.

### 3-point bending tests

3-point bending tests were performed to check to relation between deflection of the cell and the applied charge. The experimental results were compared with the numerical simulation outputs (figure 3). Two stacks of panels were tested, one with materials A and B, and the other one with material C for the front and back sheets.

The experimental bench uses supports distant of 100 mm (figure 4). 4 configurations were tested :

1. Application of the force on the **back** side of the PV cell with ribbons (Y-axis) **parallel** to the supports (Y-axis) ;
2. Application of the force on the **front** side of the PV cell with ribbons (Y-axis) **parallel** to the supports (Y-axis);
3. Application of the force on the **back** side of the PV cell with ribbons (X-axis) **perpendicular** to the supports (Y-axis);
4. Application of the force on the **front** side of the PV cell with ribbons (X-axis) **perpendicular** to the supports (Y-axis).

Preliminary tests enabled to evaluate the force level at which the first damages appear. These tests made it possible to estimate a maximum load and loading stages for the PV modules, based on samples of the same stack without an integrated cell.

For the modules, the applied displacement increased at a rate of 5 mm/s, until reaching the next force stage (by steps of 10 % of the previously determined maximum charge). The test was performed by stages to enable a dark I-V monitoring of the test with a Keithley voltage source.

The dark I-V measurement is operated on a module which is either placed in the dark or under a cover. The advantage of this method is that the electrical parameters [10] can be determined with samples undergoing bending tests, in contrast to tests such as light I-V or lock-in, which require placing the panel in a particular equipment that is not easily compatible with the bending test assembly. The Keithley device performs a voltage scan across the module terminals and records

the output current. This measurement enables to access electrical parameters of the module thanks to a routine developed by Suckow [11][12].

The experiment was stopped when the first mechanical or electrical damages were observed. The mechanical failure is noticed by listening to cracks of the structure, and is signalled by fluctuations of the force-displacement curve. When an electrical damage appears, the appearance of the dark I-V curves changes from a double diode model to a one diode model (figure 5), for the cells we use. Thus, we can detect the electrical failure of the module. As this test requires a scan, it is necessary to stop at force stages to perform the measurement. Moreover, 2 measurements were done at each force stage to ensure the repeatability of the measurement. A total of 25 tests was performed, on 5 different modules.

For each measurement, the applied force and the corresponding deflection of the module are registered and synthetized in a graph (see figure 6).

## Correlation between experimental data and numerical simulation

The deflections obtained experimentally and numerically for each level of applied force were compared (see figure 6). The simulation results show a very good correlation with experimental results for both stacks. At each stage of applied load, the relative error between the model and experiments stays within a margin of 5%. The validation of the model is the first step towards the optimization of the stack.

## Optimization of the stack

A DOE method has been led with Ellistat software to optimize the stack.

### Definition of the DOE

The aims of the DOE are to minimize the mass while reaching a rigidity equivalent to that of an automotive sheet steel. The steel plate is 0.8 mm thick, which is comparable to the thickness of a car part [13]. The steel plate and composite plates have the same dimensions: 20*20 cm.

In this first study, a 3-point bending test with supports distant of 123 mm is considered. Eventually, other loading cases will also be studied. The comparison between the two cases considers the deflection of the plates: the composite plate is expected to have a deflection smaller than or equal to that of the steel plate, which is $-3.13mm$. The initial stack of the composite plate had a deflection of $-1.51mm$: it was far too rigid.

The optimization envisaged initially included the variables and levels which can be seen in table 4.

For processing constraints, only materials A and B are used for the moment. Other materials will be used in the future. Several constraints were added, to include manufacturing and photovoltaic aspects. Indeed, as the optimized stack will be produced by an injection process, some plies of material B are mandatory for the injection process developed in the context of this study. As well, it is necessary to limit the

**Table 4 Variables of the Design Of Experiment.**

| Variable | Level 1 | Level 2 | Level 3 |
|---|---|---|---|
| Number of composite plies for the front sheet | 1 | 2 | 3 |
| Number of composite plies for the back sheet | 2 | 4 | 6 |
| Angle of each ply | $0/90^o$ | $\pm 45^o$ | |
| Thickness of the encapsulant of the front sheet | $0.3mm$ | $0.4mm$ | $0.5mm$ |
| Thickness of the encapsulant of the back sheet | $0.3mm$ | $0.4mm$ | $0.5mm$ |
| Material of the encapsulant | Material D | Material E | |

number of plies for the front sheet to choose thicknesses for the encapsulants that are available in the industry, and to maximize the Cell To Module ratio (CTM). The CTM ratio is the ratio of the output power of a solar module on the powers of all individual cells in the module: it decreases when there are optical or electrical losses.

If a complete plan of experiment is done, the complete plan would include around 8000 simulations.

### Simplification of the complete design of experiments

To ensure that our study does not involve prohibitive computation times, it was chosen to decouple some variables. Indeed, adding the angle of plies variable induces a high number of variables: one per ply, with two levels for each one.

*Choice of the number of plies*

A first study was led to reach a pre-target deflection by adapting only the number of plies for the stack. This greatly reduced the number of plies: 2 for the front sheet and 3 for the back sheet gave approximately the target deflection keeping all the other parameters as they were in the initial stack.

*DOE on the angles of plies*

Another study evaluated the influence of the impact of the angles of the plies on the deflection for this second stack: this variable has a very low influence on the final deflection of the module, in the case of this stack: the difference of deflection between the best and the worst stack is about $0.045mm$ for this structure with 5 plies which angle switches between $0/90^o$ and $\pm 45^o$. This could be partly explained by the relative thickness of the encapsulant, which acts as a core in a sandwich structure, and by the relative symmetry of the stack. After this second study, it was decided to put aside the angle of plies variable, and keep all plies at $0/90^o$, which seemed to slightly maximize the rigidity.

*DOE on the thicknesses and materials of encapsulants*

The former analyses enabled to fix the number and angles of plies. The last variables of the DOE were:

- The thickness of the front and back encapsulants, with 3 levels for each of these two variables;
- The material of the encapsulant: either material D, or E.

For each material of the encapsulant, the complete design of experiments on the thickness of the front and back encapsulants implied 9 simulations. In absolute, we have an infinite number of couples "front thickness/back thickness" reaching the

target deflection. However, from a practical point of view it has no sense because we only have 3 thicknesses of material available in the industry. Therefore, the parameters can actually only take 3 thickness values. Moreover, we imposed another criterion: the cell needs to be as close as possible of the neutral fibre. For each type of encapsulant (D or E), an optimal was found. The steps of the optimization process and intermediary results can be seen in table 5. This optimization process enabled to reduce by about 30% the mass of the module compared to the initial stack. The optimized stack is 2.7 times lighter than a steel plate with equivalent rigidity (figure 7).

**Table 5 Optimization of the mass of the module.**

| Configuration | Deflection | Mass | Thickness |
|---|---|---|---|
| Reference steel plate | $-3.13mm$ | $314g$ | $0.8mm$ |
| Composite PV panel non optimized | $-1.51mm$ | $148g$ | $2.82mm$ |
| Composite PV panel optimised with encapsulant D | $-3.05mm$ | $122g$ | $2.34mm$ |
| Composite PV panel optimised with material E | $-2.94mm$ | $113g$ | $2.18mm$ |

## Conclusion

A predictive model of the mechanical behaviour of a composite structure with integrated photovoltaic cells was designed. It was validated through 3-point bending tests measurements, with a relative error of around 5% with experimental data.
The predictive model allowed to optimize the composite layout of the laminate structure integrating the PV cells playing on the materials, thicknesses of the plies, and angles of the plies.
The resulting structure is also pre-qualified with standard photovoltaic qualification equipment, including spectrophotometry, electroluminescence and I-V measurements before and after tests in climatic chambers (norm IEC 61215). They enable to evaluate and optimize the power supply of the panel, choosing the most appropriate materials for the front sheet.
This work enabled the research team to size a PV module with composite front and back sheets.
The next steps include :

- Adding thermomechanical properties to the model to simulate thermal cycling and the deformation of the piece after processing it at high temperature, e.g. by a thermocompression compress;
- Performing a DOE on the stack to minimize residual stress after thermocompression;
- Study double-curved composite modules integrating PV cells, especially to predict the risk of breaking the cells with this geometry. This curved structure would be more representative of the shape of automotive car parts.

**Availability of data and materials**
The datasets used and/or analysed during the current study are available from the corresponding author on reasonable request.

**Competing interests**
The authors declare that they have no competing interests.

**Author's contributions**
T. Duigou, J. Gaume, M. Lagache and P. Saffré developed the theory, conceived and carried out the experiments. T. Duigou performed the simulations and wrote the manuscript with inputs from all authors. All authors provided critical feedback and helped shape the research and analysis.

**Funding**
This work is financed equally by CEA and IPC.

**Acknowledgements**
The authors would like to acknowledge Vincent Boichon (IPC), Lucas Douchin, Lucas Feliciano, Aurélie Guillou (Polytech) and Hervé Robin (CEA) for their contribution to the experimental tests and characterization of samples, and Xavier Brancaz, Gilles Dennler (IPC), Pascal Francescato and Maurice Pillet (SYMME) for the scientific support.

**Author details**
[1]Université Grenoble Alpes, CEA, LITEN, DTS, SMPV, LMPI, INES, F-38000 Grenoble, France. [2]SYMME, Univ. Savoie Mont Blanc, FR 74000 Annecy, France. [3]Centre Technique Industriel de la Plasturgie et des Composites (IPC), 01100 Bellignat, France.

**References**

1. Araki, K., Ji, L., Kelly, G., Yamaguchi, M.: To do list for research and development and international standardization to achieve the goal of running a majority of electric vehicles on solar energy **8**(7), 251. doi:10.3390/coatings8070251. Accessed 2019-02-13
2. González, C., Vilatela, J.J., Molina-Aldareguía, J.M., Lopes, C.S., LLorca, J.: Structural composites for multifunctional applications: Current challenges and future trends **89**, 194–251. doi:10.1016/j.pmatsci.2017.04.005. Accessed 2019-02-22
3. Amalu, E.H., Hughes, D.J., Nabhani, F., Winter, J.: Thermo-mechanical deformation degradation of crystalline silicon photovoltaic (c-si PV) module in operation **84**, 229–246. doi:10.1016/j.engfailanal.2017.11.009. Accessed 2019-05-06
4. Eitner, U.: Thermomechanics of Photovoltaic Modules
5. Dietrich, S., Pander, M., Sander, M., Schulze, S.H., Ebert, M.: Mechanical and thermomechanical assessment of encapsulated solar cells by finite-element-simulation, p. 77730. doi:10.1117/12.860661. http://proceedings.spiedigitallibrary.org/proceeding.aspx?doi=10.1117/12.860661 Accessed 2019-09-10
6. Hasan, O., Arif, A.F.M., Siddiqui, M.U.: Finite element modeling, analysis, and life prediction of photovoltaic modules **136**(2), 021022. doi:10.1115/1.4026037. Accessed 2019-09-10
7. Gay, D.: Matériaux Composites, 4e édition edn. Hermes Science Publications
8. Damiani, O.: Procédure Technique de L'outil de Simulation Mécanique ANSYS
9. Krawczak, P.: Essais des plastiques renforcés **AM5405 V1**, 44
10. Breitenstein, O.: Understanding the current-voltage characteristics of industrial crystalline silicon solar cells by considering inhomogeneous current distributions (3), 24
11. Suckow, S., Pletzer, T.M., Kurz, H.: Fast and reliable calculation of the two-diode model without simplifications: Fast and reliable calculation of the two-diode model without simplifications **22**(4), 494–501. doi:10.1002/pip.2301. Accessed 2020-03-24
12. Suckow, S.: Manual for Program \2/3-Diode Fit"
13. Virolle, J.-B.: Les Aciers Utilisés dans les Tôles Automobiles. https://metalblog.ctif.com/2019/01/14/les-aciers-utilises-dans-les-toles-automobiles/

**Figures**

**Figure 1 Stack of the PV module.** On the right is a cut in thickness of the stack. Depending on the position in the plane, the material may change, e.g. copper ribbons or EVA are just above the cell depending on the position. On the right is a top view of the one-cell composite module.

**Figure 2 Tensile curves for material C.** On the left are the complete curves, and on the right a zoom on the most linear part of the curves.

**Figure 3 Simulation of the deformation of the module under 3-point bending test.**

**Figure 4 Bench and global coordinates for the 3-point bending test.**

**Figure 5 Detection of an electrical damage with dark I-V.** When an electrical damage appears, the curve switches from a double-diode model to a one-diode model.

**Figure 6 Correlation between the force-displacement curves for stack with material C.** The linear regression analysis uses the least-squares method and minimizes the sum of squares of deviation of data points from the line. The correlation between the experimental measurements (5 modules) and the simulation is very good: the relative error stays within a margin of $5\%$.

**Figure 7 Optimization of the composite PV panel mass compared with a reference steel plate.**

# Figures

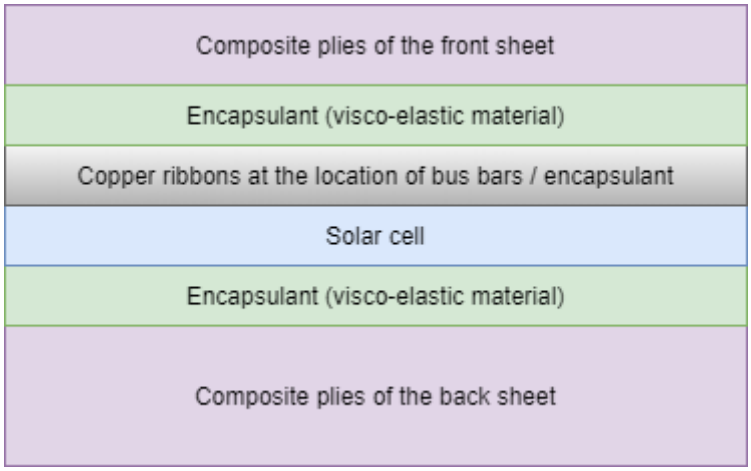


**Figure 1**

Stack of the PV module. On the right is a cut in thickness of the stack. Depending on the position in the plane, the material may change, e.g. copper ribbons or EVA are just above the cell depending on the position. On the right is a top view of the one-cell composite module.

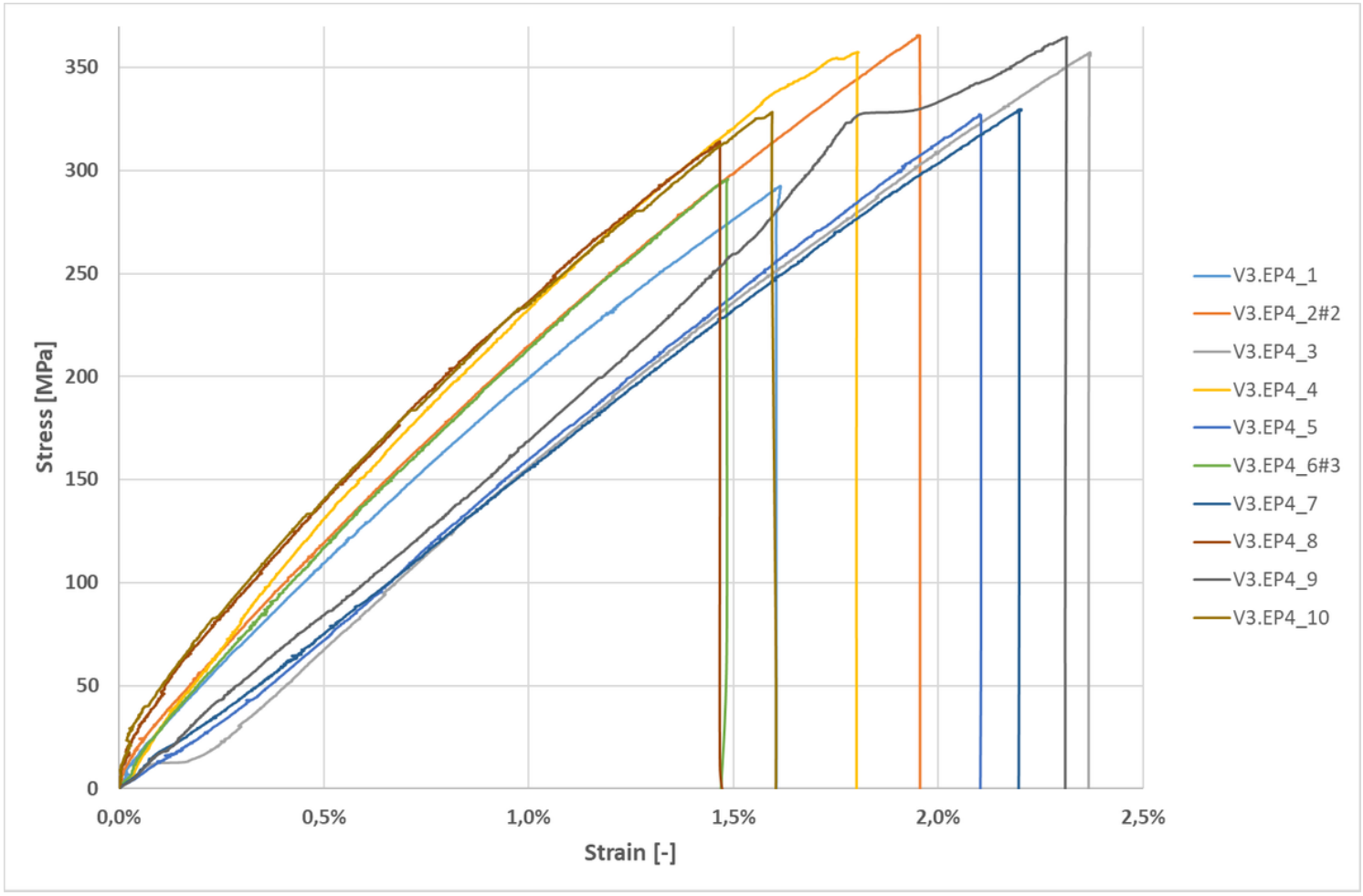


**Figure 2**

Tensile curves for material C. On the left are the complete curves, and on the right a zoom on the most linear part of the curves.

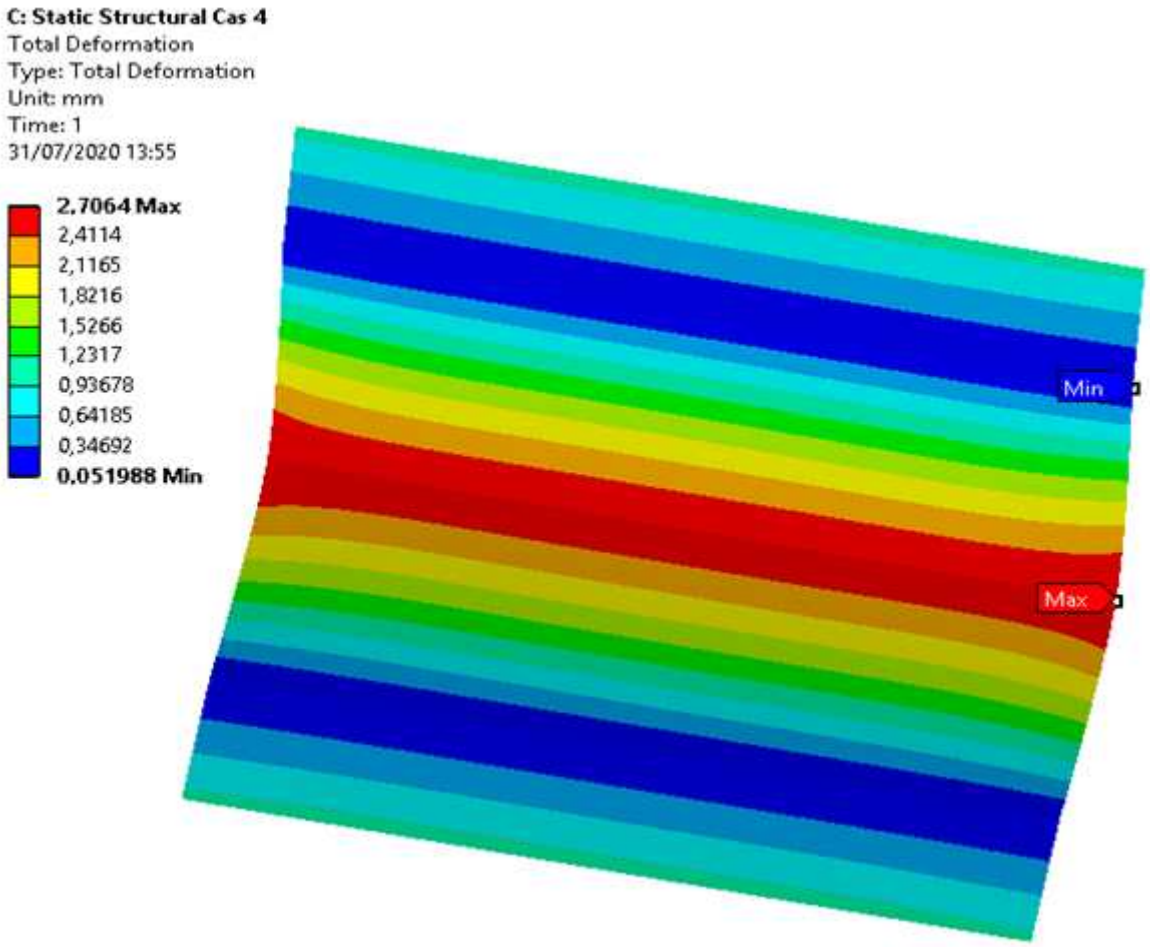


**Figure 3**

Simulation of the deformation of the module under 3-point bending test.

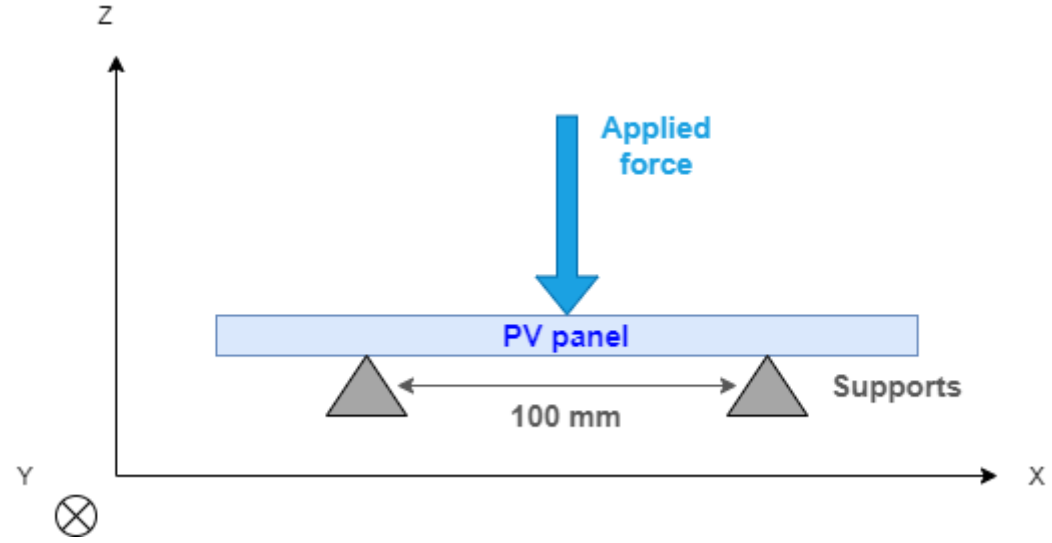


**Figure 4**

Bench and global coordinates for the 3-point bending test.

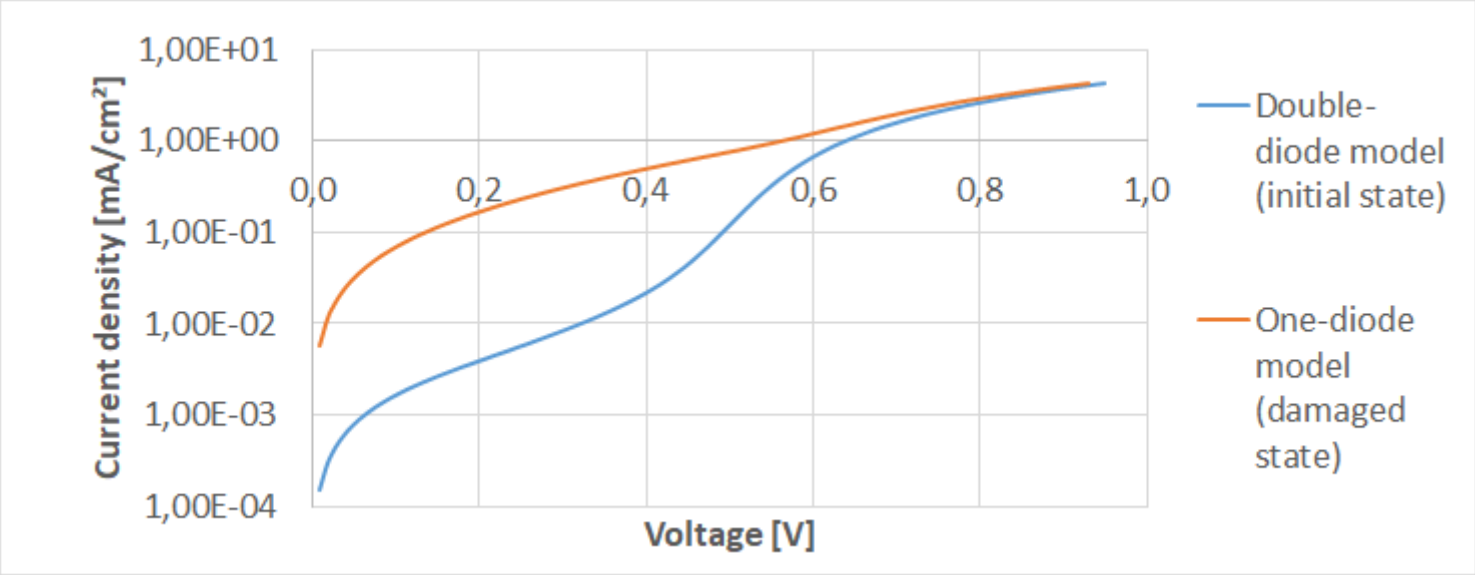


**Figure 5**

Detection of an electrical damage with dark I-V. When an electrical damage appears, the curve switches from a double-diode model to a one-diode model.

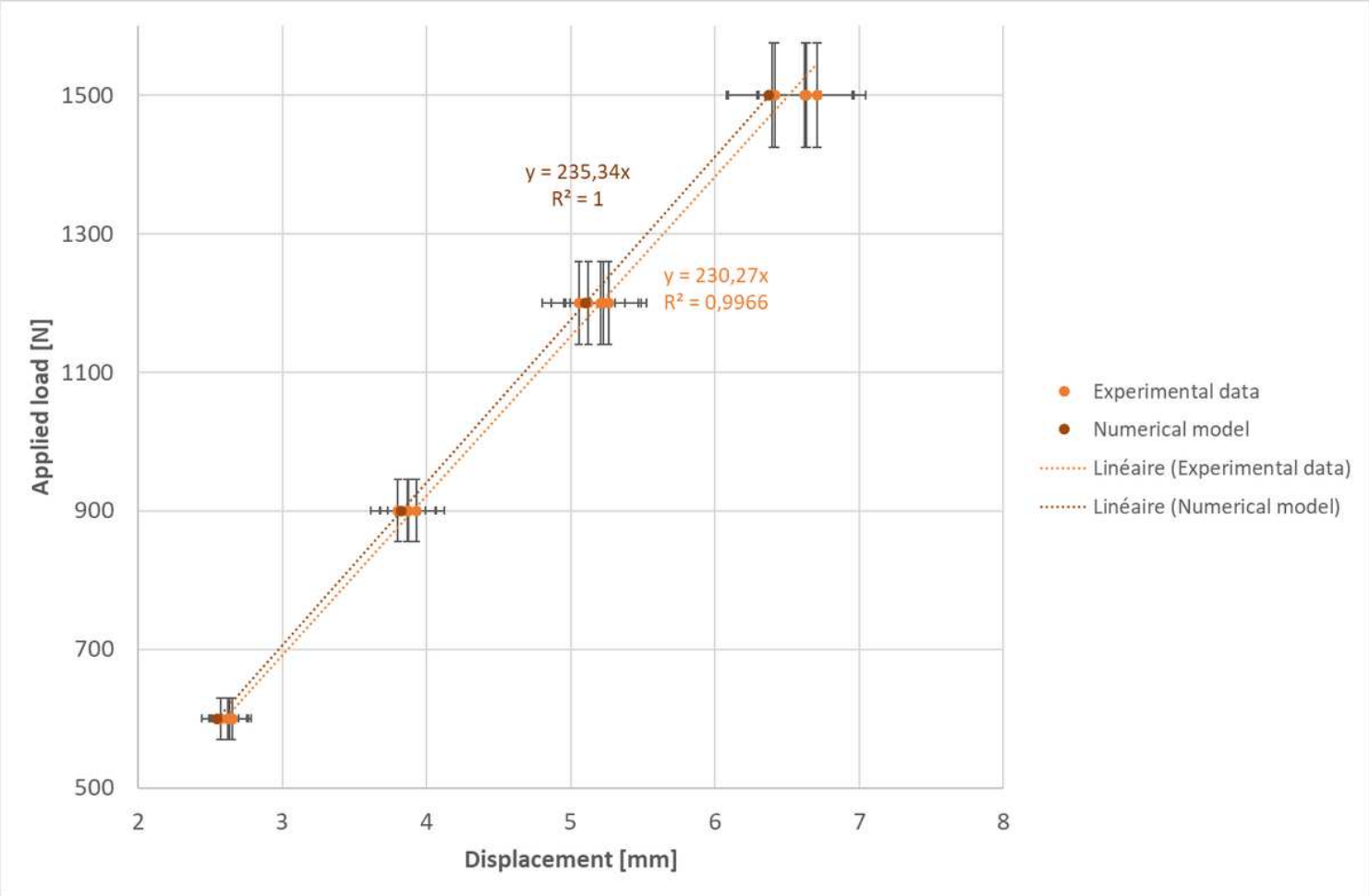


**Figure 6**

Correlation between the force-displacement curves for stack with material C. The linear regression analysis uses the least-squares method and minimizes the sum of squares of deviation of data points from the line. The correlation between the experimental measurements (5 modules) and the simulation is very good: the relative error stays within a margin of 5%.

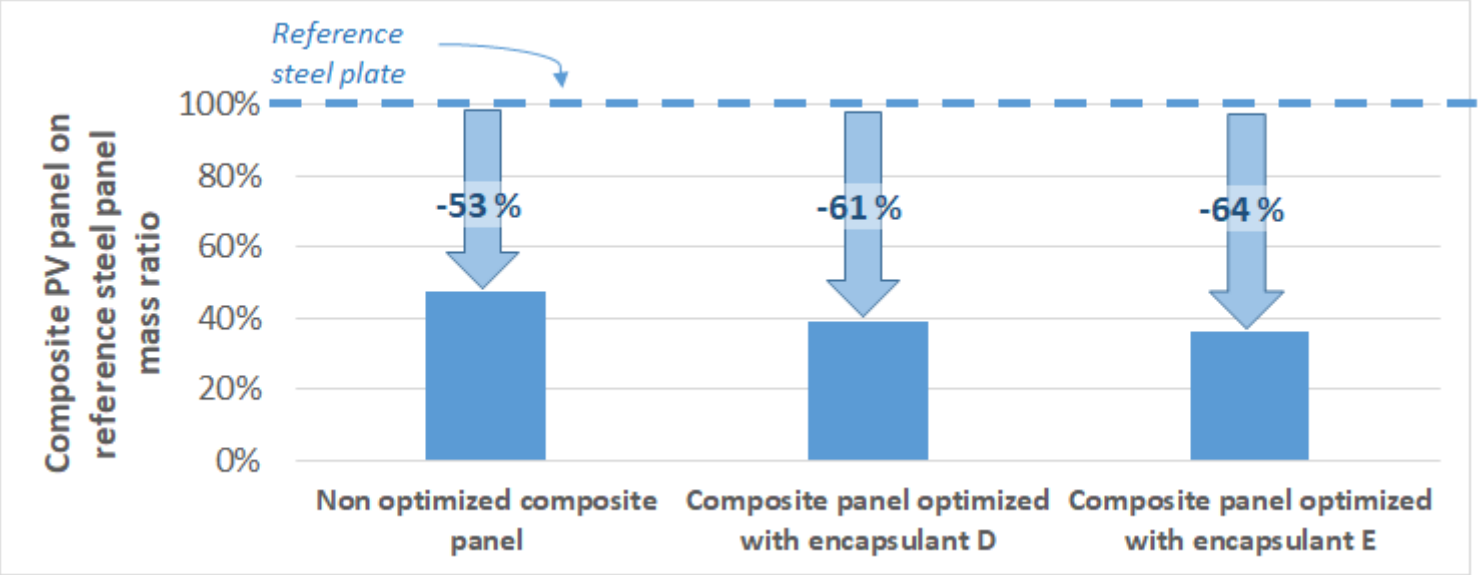


**Figure 7**

Optimization of the composite PV panel mass compared with a reference steel plate.